

Pilot System for Light-Weight Precision Gravimeter

¹A.S. Aguib, ²I. El Sebaie and ³A. Mohamed

¹El Shorouk Academy, the Higher Institute of Engineering, Egypt

²College of Engineering, King Saud University, Saudi Arabia

³Geomatics USA, Limited Liability Company, United States of America

Abstract: Gravity measurements are required for many applications. Examples of which are; monitoring of ground water depth changes and determination of the Geoid (Extension of Mean Sea Level MSL under the solid Earth) are among the important data used in many engineering applications. Commercially available precision gravimetry systems that use proprietary accelerometers are bulky, expensive and not easily integrate-able in vehicle mountable systems. In this research low expensive light weight accurate system is designed based on a navigation-grade, GNSS-aided inertial navigation system and a low-noise seismic accelerometer triad sensor. It can be mounted on a vehicle to measure accurate real time gravity differences among points. The system is tested and preliminary results reveal 1 μ Gal (1 micro-gal) potential gravity anomaly estimates. The developed system can be used in applications as mapping groundwater depth change by correlating it with the measured gravity anomalies to combat groundwater depletion.

Key words: Precision Gravity System • Accelerometer • Navigation System • GPS • Depletion

INTRODUCTION

As groundwater depletion becomes a global problem [1]. Many places in the world like the Kingdom of Saudi Arabia are in dire need of utilizing its vast underground resources, including groundwater, for development. Understanding earth's subsurface structure is important at global, regional and local scales for groundwater discovery, oil and gas exploration, mining and subsurface feature identification [2]. Adequate mapping of resources provide best management practitioners for better informative decision making. For instance, groundwater is considered as the main source of water within the rural and urban regions within the Kingdom of Saudi Arabia.

Mapping of underground resources, however, cannot be carried out adequately by conventional techniques used in remote sensing and photogrammetry. Methods of geophysical gravity provide a way of estimating changes within the water storage's subsurface [3]. This can be achieved through carrying out measurements of the changes which are observed in gravitational field of earth. It has been revealed that the ocean loading effects, polar motion, mass changes within the atmosphere and solid Earth's tides primarily influence temporal changes within the gravity field of Earth.

According to the studies of Creutzfeldt *et al.* [1], Christie *et al.* [2], Hannah *et al.* [4], Maurer *et al.* [5] and Watson *et al.* [6] it is revealed that observations of gravity enable the determination of entire hydrological system responses. The research has further claimed the fact that if the effects of ocean tides and Earth, polar motion as well as atmosphere are neglected, then the remaining response is controlled by variations or changes in hydrological mass. Changes within the water storage in the locality of sensor cause these changes or variations in gravity.

The sequential gravity surveys might also be carried out with the help of satellites for measuring changes within the groundwater storage accurately and efficiently over huge regions [7]. According to Jacob *et al.* [8] it is found that gravity signal is also used in Larzac Plateau in Southern France in a karst for the detection of groundwater. Hence, it can be said that this approach encompasses the potential of offering near real time monitoring as well as evaluation of subsurface hydrologic variations. As a result of these measurements and assessments, water managers can respond accordingly. According to Pool *et al.* [9] detecting groundwater using the gravity signal was implemented to the Tucson Basin in USA in southern Arizona.

The study of Niu [10], Seo [11] and Swenson *et al.* [12] found that in situ hydrological observational data and that inferred from the GRACE (Gravity Recovery and Climate Change Experimental) Experiment satellite mission data agree to 20 mm (Rmse) with the use of a filtering technique to improve the spatial resolution [13]. High resolution density variations beneath the earth surface, when viewed spatially, offer an intuitive means for characterizing the structural makeup of the earth's subsurface [14]. Nano seismic accelerometers offer low-noise gravity sensor with shorter spatial resolution achievable through GRACE. According to Pinto *et al.* [15] when combined with observational data from GPS (Global positioning system) and tactic grade inertial navigation system, gravity anomaly recovery at the few milliGals level is achievable. These effects of gravity need to be eliminated so as to expose the hydrological signal within the measurements of gravimeter [8]. Consequently, high resolution ground water storage variation detection becomes more accurate and more reliable.

Sensors used in previous work are bulky and heavy. They are not suitable for light-weight micro or mini unmanned autonomous systems. This research enables wide area gravimetry mapping through the use of new nano-technology sensors for precise relative navigation, innovation in data processing and affordable carrier platforms to both reducing cost and producing finer spatial resolution. In this project a custom built light-weight and highly-sensitive gravimetry system is designed to be suitable for measuring gravity anomalies in environment such as of Saudi Arabia. The system is our tool to acquire gravimetry data, used alongside pre-knowledge of mapped area, to develop hydrological models that correlate groundwater storage change with gravity anomaly [16]. The system built uses state-of-the-art space and aeronautical global positioning-aided inertial navigation system and nano-technology-based accelerometer triads for low-noise measurements. The project provides a platform to the Saudi researchers to further harness their skills in the area of field data acquisition and analysis, not only in water management, but also in other related areas such as oil and gas exploration.

Approach: The approach followed in this research includes several steps. First is to identify the theoretical bases for the idea including the representing mathematical model. Then next step is discussing and defining the sources of possible errors with the related equations, that could be used for error elimination or reduction. Following is choosing the required hardware components for

constructing the Grav-Map device for gravity anomaly measurements. Next is the design of the software that will synchronise the data collected and provide the final gravity readings. Last is the lab testing of the device and determining the expected measured gravity accuracy. Field testing and correlating with groundwater depths discussion and evaluation can be found in another paper by El Alfy *et al.* [17]. This paper is intended to show the possibility and how to construct and test a light weight and low cost gravimeter basing on new measuring idea through using three main components. They are Inertia Measuring Unit IMU, Accelerometer and Global Positioning System GPS. The proposed system succeeded in realising a reasonable consistent measuring accuracy of 1 μ Gal.

MATERIALS AND METHODS

A methodology developed through a National Science Foundation funded research (NSF Solicitation 09-541: Topic IC3.I.ii) is sought to be further developed in this research to cover the requirements to construct and test a practical innovative gravity system that is mountable onboard a moving land-based vehicles or aircraft. The proposed system is expected to include three main components; GNSS receiver board, Inertial Measurement Unit (IMU) and Accelerometer triad.

Mathematical Modeling

Gravimetry Sensing: The first step is to identify all the factors that affect the upward component of the scalar gravity disturbance in the Earth's gravitational field. This can be modeled using Newton's equation of motion. According to Bruton *et al.* [3], Glennie [14], Jekely [18], Mohamed [19], Schwarz and Wei [20] and Wei and Schwarz [21] the disturbance is calculated from two streams of acceleration information, a stream including the gravity like inertial accelerometer and the other is gravity-free like Global Positioning System (GPS). This can lead to the following relation:

$$\delta g = f_u - a_u + E_c + \gamma_u \quad (1)$$

where,

δg upward component of the *Scalar gravity disturbance* in the Earth's gravitational field. It is measured in mGal (Milli Galileo) where 1 mGal \sim 1 μ g = 10⁻⁵ m/s² and g is considered as the average gravity acceleration of Earth which is approximately 9.81 m/s²).

- f_u upward component of the specific force,
- a_u upward component of the vehicle acceleration,
- γ_u upward component of the normal gravity vector at vehicle height,
- E_c Eötvös correction due to Coriolis and centrifugal accelerations in the horizontal plane.

Gravimetry Sensing Sources of Errors: The next step in the procedure is to find out the sources of errors and its calculating equations. Equation (1) above shows two main sources of errors: specific source measurement errors and vehicle's acceleration computation error.

Specific Source Measurement Errors: Since the specific force is measured within the body frame and not within the local level frame, a transformation matrix is required to map such measurement between the frames [22]. Such mapping results in the following errors:

The leveling misalignment errors due to the coupling of the leveling misalignment gyroscopic errors and the measured horizontal accelerometer specific force, which can be expanded in scalar form F_ϵ^b to:

$$F_\epsilon^b \mathbf{e} = f_E \mathbf{e}_N - f_N \mathbf{e}_E \tag{2}$$

where,

- f_E, f_N Specific force measurements within the east and north directions,
- $\mathbf{e}_E, \mathbf{e}_N$ Misalignment errors in the east and north directions.

The specific force errors due to the accelerometer specific force measurement error mapped onto the upward direction, the second term of (2) which after expansion is reduced to.

$$R_b^l df_b = -\cos\theta \sin\phi df_x + \sin\theta df_y + \cos\theta \cos\phi df_z \tag{3}$$

where,

- df_x, df_y, df_z Accelerometer specific force measurement errors in the x-, y-, z-body frame directions,
- θ, ψ, ϕ roll, heading angles and pitch of vehicle on the basis of following transformation matrix between the local-level frame and the body frame:

$$R_b^l = R_3(-\psi)R_1(-\theta)R_2(-\phi) = \begin{pmatrix} \cos\psi\cos\phi - \sin\psi\sin\theta\sin\phi & -\sin\psi\cos\theta & \cos\psi\sin\phi + \sin\psi\sin\theta\cos\phi \\ \sin\psi\cos\phi + \cos\psi\sin\theta\sin\phi & \cos\psi\cos\theta & \sin\psi\sin\phi - \cos\psi\sin\theta\cos\phi \\ -\cos\theta\sin\phi & \sin\theta & \cos\theta\cos\phi \end{pmatrix} \tag{4}$$

The time synchronization error is due to the shift (And possibly jitter) of the IMU time keeping relative to GPS. Starting with equation (2) and differentiating both sides with respect to time, we get.

$$\frac{df_u}{dt} = \dot{R}_b^l f_b + R_b^l \dot{f}_b \text{ or } df_u = (\dot{R}_b^l f_b + R_b^l \dot{f}_b) dT \tag{5}$$

where,

- df_u upward acceleration error
- dT time synch error between IMU and GPS signals
- R_b^l third row of the transformation matrix $R_b^l = [-\cos\theta\sin\phi\sin\theta\cos\theta\cos\phi]$
- \dot{R}_b^l rate of change of the transformation matrix, the maximum of which (Assuming small leveling angles) is $\max(\dot{R}_b^l f_b) = 2\dot{\theta}f_x + 2\dot{\theta}g$
- f_b, \dot{f}_b body specific force measurements and their time rates, the maximum of which is

$$\max(R_b^l \dot{f}_b) = \dot{f}_z$$

Vehicle's Acceleration Computation Error: This error is due to the vehicle's acceleration as computed from a gravity-free sensor like GPS. Vehicle acceleration can be computed by differentiating GPS velocity once or by differentiating GPS position twice [8]. Assuming constant acceleration dynamics,

$$da_u = 0 \text{ or } da_u = \frac{dv_u}{dt} \text{ or } da_u = \frac{d^2 p_u}{dt^2} = \frac{2dp_u}{dt^2} \tag{6}$$

where,

- dp_u, dv_u, da_u vehicle's position, velocity and acceleration upward component errors as computed from GPS carrier phase or carrier phase rate measurements,
- dt Integration time period.

Eötvös correction computation error (E_c error) is due to Coriolis and centrifugal accelerations in the horizontal plane and is computed as follows:

$$E_c = 2v_E \omega_e \cos\phi + \frac{v_E^2}{R_1 + h} + \frac{v_N^2}{R_2 + h} \tag{7}$$

its linearized form,

$$dE_c = 2v_E \left\{ -(\omega_e \sin \varphi) d\varphi + \left(\frac{\omega_e}{v_E} \cos \varphi + \frac{\left(1 + \frac{v_N}{v_E}\right)}{R+h} \right) dv_E \right\}$$

In which,

- ω_e Earth's rotation rate ($\sim 15^\circ/h = 7.29 \times 10^{-5}$ rad/s),
- v_E, v_N east and north components of the vehicle's velocity,
- φ, h Vehicle geodetic latitude and ellipsoidal height,
- R_1, R_2 Earth's prime vertical and meridian radii of curvature ($R \sim 6,378$ km - WGS84 ellipsoid.)

The main contributor of the *Eötvös* error is the vehicle's measured velocity by GPS carrier phase or carrier phase rate.

The Normal gravity computation error ($d\gamma_u$ error) depends on the normal gravity model used and is a function of the vehicle position, specifically its height above the reference ellipsoid [23]. It can be approximated by the following:

$$d\gamma_u = \frac{2\gamma_u}{R} dh \tag{8}$$

where,

- dh vehicle's height error as obtained from GPS carrier phase measurement
- γ average value of the normal gravity (~ 9.81 m/s²)
- R Earth's mean radius of curvature (6,378 km for the WGS84 datum.)

System Overview: The developed system to acquire gravimetry data in this project is called Grav-Map (Figure 1) with a dimension of 15x15x15 cm and weight of 2 kg for the main body. There are cables to connect with computer and external 12-volt 2-Amp battery.

System Hardware: The Grav-Map gravimetry system consists of five major components as follows:

- Single-board computer
- GNSS receiver board
- Inertial Measurement Unit (IMU)
- Accelerometer triad and
- Communal power and interface board.

Data flow between the components is shown in Figure 2.



Fig. 1: The Grav-Map System in a Carrying Case

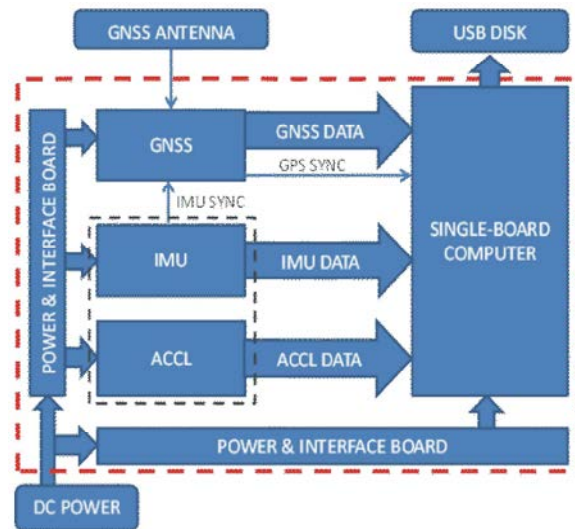


Fig. 2: Data flow (Including synchronizing signals) among components. Red dashed box represents the system enclosure. Black dashed box refers to the fact that IMU and accelerometer are physically outside the system enclosure but connected to the single-board computer through a communal cable [24]

Table 1 shows the component details of the Grav-Map as well as the manufacturer part number.

Table 1: Grav-Map System Components

Part	Manufacturer	Description	Part number
GNSS Antenna	Antcom, California	Active L1/L2 GNSS Antenna, 3.5"	3G1215A
Accelerometer	Colibrys, Switzerland	three axis combination of SF1600 Si-Flex™ MEMS analog capacitive accelerometers	SF3600.A
IMU	Memsense, South Dakota	H3 High Performance 6 DOF IMU	HP02-0150F050R
Enclosure	Geomatics USA, Florida	Custom 4"x4"x4" with mounting base, DB15 and SMA communication interface and ACCEL and IMU LED indicators	GravMap-SHE03

Three peripheral connections are used for 1) GNSS antenna connection, 2) input DC power and 3) data storage, which is a generic USB disk that also contains startup configuration scripts for the system.

Software: The software developed for the Grav-Map device includes two parts, the first runs on the single-board computer for acquiring data from the GNSS receiver board, the IMU and the accelerometer, including the synchronization (Time-stamping) mechanism of acquired data [5]. The other is the post-processing software that translates/converts the acquired signal into readable data formats.

Data Acquisition Program: Upon initialization, the main function installs an interrupt routine for acquiring data from the GNSS receiver board, the IMU and the accelerometer. The interrupt routine is triggered externally by the 1-Hz pulsing signal from the GNSS receiver board [10]. The routine timestamps GNSS time, IMU frame count and accelerometer data with computer time for further synchronization in post-processing and then reads and saves all data from buffer to disk.

Data Post-Processing Programs: The acquisition software saves data in binary format and keeps timestamps in computer time without actually performing synchronization between computer time, GNSS time and IMU frame count in order to maintain high data rate in acquisition time [9]. The processing software is then used to convert/translate the binary data into readable data format. The processing software contains the following functions:

- ConvertGNSS: to convert binary RTCM3 data to standard RINEX data format
- ConvertIMU: to convert binary IMU data to TEXT file with pulsing information [15]
- ExtractEvent: to extract IMU pulsing information (i.e. GNSS event markers) in GNSS time from binary GNSS data

- SyncIMUtime: to time-stamp IMU data with GNSS time by searching and interpolating IMU pulsing information in GNSS time [11].

Accelerometer data is already saved in TEXT format and time-stamped with GNSS time [25]. The output of the processing software is TEXT files that include GNSS range measurements in RINEX format, IMU velocity increments and angular rates time-stamped in GNSS time and accelerometer velocity increments time-stamped in GNSS time [12]. In other words, at any given GNSS time, there are range values with orientation, which will be further processed to produce the platform trajectory, along with the accelerometer data for recording gravity values [20] Figure (3).

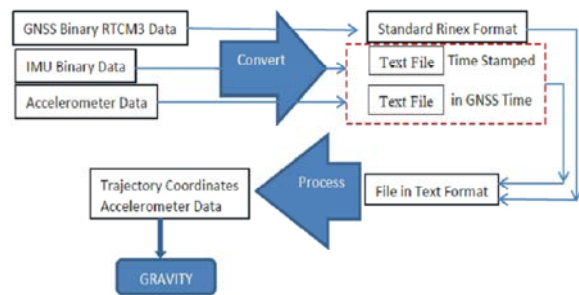


Fig. 3: Flow Chart of Post Processing Software Steps and Outputs

System Testing

Platform Leveling Errors: Leveling error is a function of the initial misalignment -which is a function of the Accelerometer bias- and the Gyro drift bias. In free inertial navigation mode, leveling misalignment grows sinusoidal but it is bounded by the Schuler oscillation [26]. A simplified inertial navigation model as the one in Mohamed [19] and Savage [25].

$$\delta \dot{v} = g\epsilon + b \text{ and } \dot{\epsilon} = -\frac{\delta v}{R} + d \tag{9}$$

Solving the above first-order differential equations, the maximum leveling misalignment will be:

$$\max(\epsilon) = b_1(2\cos\beta_{\max} - 1) + d_1 \sin\beta_{\max}$$

where,

b_1, d_1 Relative Accel and Gyro drift biases

$$b_1 = -\frac{b}{g} \text{ and } d_1 = \frac{d}{v}$$

where $d_1/b_1 \sim 5$ for most tactical-grade and navigation-grade IMUs

b, d Absolute Accel and Gyro drift biases

g, v Earth's gravity acceleration ($\sim 9.81 \text{ m/s}^2$) and Schuler frequency (1/5000 Hz)

β_{\max} Angle at maximum leveling error, which occurs at

$$\beta_{\max} = \tan^{-1}\left(\frac{d_1}{2b_1}\right)$$

For IMUs that maintain the above ratio between the Gyro drift bias and the Accelerometer bias, the gyro drift bias dictates the maximum leveling misalignment error [21]. Therefore, we can approximate the maximum leveling misalignment error as,

$$\epsilon_{\max} \sim 0.85d_1 \sim \frac{0.85d}{v} \sim \frac{d}{290} \Rightarrow \epsilon_{\max} \sim 3.45d^{\circ/h} \text{ mrad}$$

In GPS-aided inertial mode, the Schuler oscillation breaks and leveling misalignment error grows between the GPS updates only [25]. Based on the simplified error model above, it can be easily shown that the misalignment error can be calculated as:

$$\epsilon_{\text{GPS}} = \epsilon_0 + \tau d + \text{RW}_{\text{GPS}}$$

where,

ϵ_0 initial leveling misalignment and is equal to the relative Accelerometer bias $\epsilon_0 = b_1 = \frac{b}{g}$

d absolute Gyro drift bias

τ time between (GPS velocity) updates

RW_{GPS} Random walk of the (GPS velocity) white noise the variance of which grows with time as

$$\sigma_{\text{RW}}^2 = \left(\frac{\sigma_{\text{VGPS}}}{R}\right)^2 \tau t$$

where, t is the elapsed time since the beginning of the mission and R is considered as the mean Earth's radius which is approximately 6,378,000m

The GPS velocity can be shown to have minimal effect in normal operation during noise random walk as: For a $1^\circ/h$ and 1 mg IMU, $\epsilon_0 = b_1 = 1 \text{ mrad}$ and $\tau d = \frac{10}{3600} \times 1 = 0.003^\circ = 0.05 \text{ mrad}$ (For $\tau = 10 \text{ sec}$); For a $\sigma_{\text{VGPS}} = 0.01 \text{ m/s}$, $\sigma_{\text{RW}} = \left(\frac{0.01}{6378000}\right) \times \sqrt{10 \times 7200} = 0.0004 \text{ mrad}$ after two hours of operation.

Also, the Gyro drift bias will have minimal effect under frequent GPS updates of 100 seconds or less [26]. Therefore, the maximum leveling misalignment in this case is a function of the Accelerometer bias (not the gyro drift bias), i.e. $\epsilon_{\max} \sim \epsilon_0 \sim b_1 \sim b/g$.

The worst case scenario of equation (9) is when all errors add up. Leveling angles are usually small during gravimetric flights [24]. Taking the small angle assumption and assuming that all accelerometers will have the same noise level, Equation (9) reduces to,

$$\max(R_b^l df_b) = \max\left(\cos^2\theta - \frac{1}{2}\sin(2\theta) + \sin^2\theta\right) df_z = kdf_z = \text{accelerror}$$

Coefficient 'k' above will not exceed one for all leveling angles (roll and pitch) between 0° and 90° [4]. If the Accelerometer noise is high at the data rate, further filtering of the data at a lower frequency should bring the effect of this error down.

$$\max\left(R_b^l df_b\right) = kdf_z = b$$

K , however, exceeds one (with a maximum value of about 1.75) for leveling angles larger than 90° ; Figure 4. This case is unlikely to occur in mobile gravimetry.

Analog to Digital Quantization Noise: 16 bit ADC with theoretical quantization noise of $\sigma_q = \frac{q}{\sqrt{12}}$, where the

quantum 'q' is calculated as: $q = \frac{\text{inputrange}}{\#\text{quanta}} = \frac{\pm 5V / (1.2V.g)}{2^{16}} = 127\mu\text{g}$, leading to a quantization

noise of $\sigma_q = \frac{127}{\sqrt{12}} = 37\mu\text{g}\sqrt{\text{Hz}}$. At a digitization rate of 100

KHz, $\sigma_q = \frac{37}{\sqrt{100,000}} = 0.1\mu\text{g}$ i.e. 0.1 micro-g rms.

The main gravimetric use of the GNSS receiver board is to model the platform motion [5]. The acceleration noise (1-sigma) introduced by 0.1 mm positional error at 20 Hz sampling rate ($\Delta t = 1/20 \text{ s} = 50 \text{ ms}$) over a filtering period of 5 seconds (a spatial resolution of 500 m for a vehicle moving at 100 m/s speed) is:

$$\sigma_a = \sqrt{\frac{20\Delta t}{T^5}} \sigma_p = \sqrt{\frac{20 \cdot \frac{1}{20}}{5^5}} * 0.0001 = 1.8 * 10^{-6} \frac{m}{s^2} = 0.2 \mu g$$

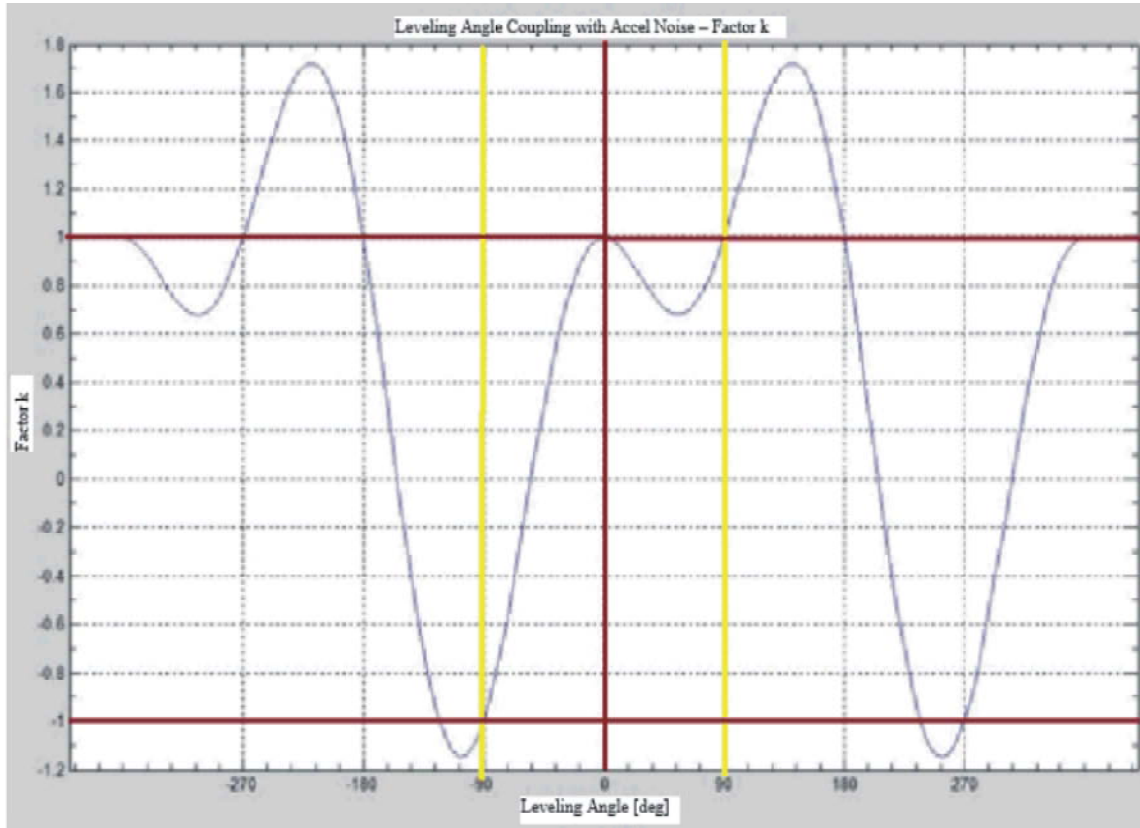


Fig. 4: Leveling Angles Coupling Factor (k)

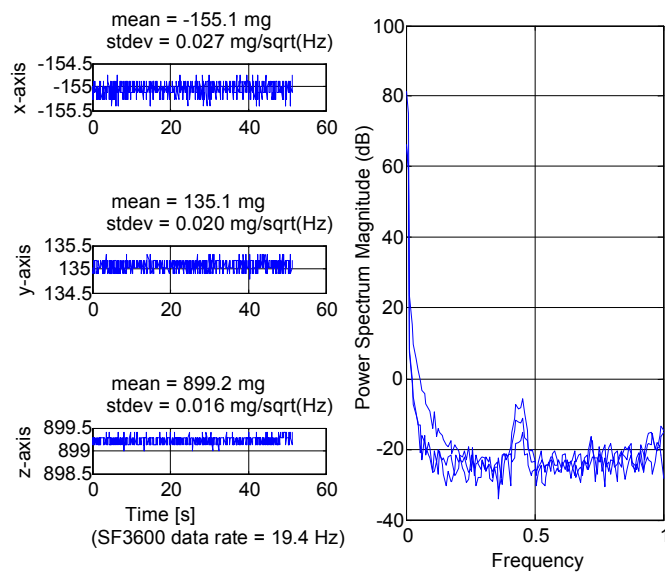


Fig. 5: Short-Term Noise And Spectrum Of The Acquired Accelerometer

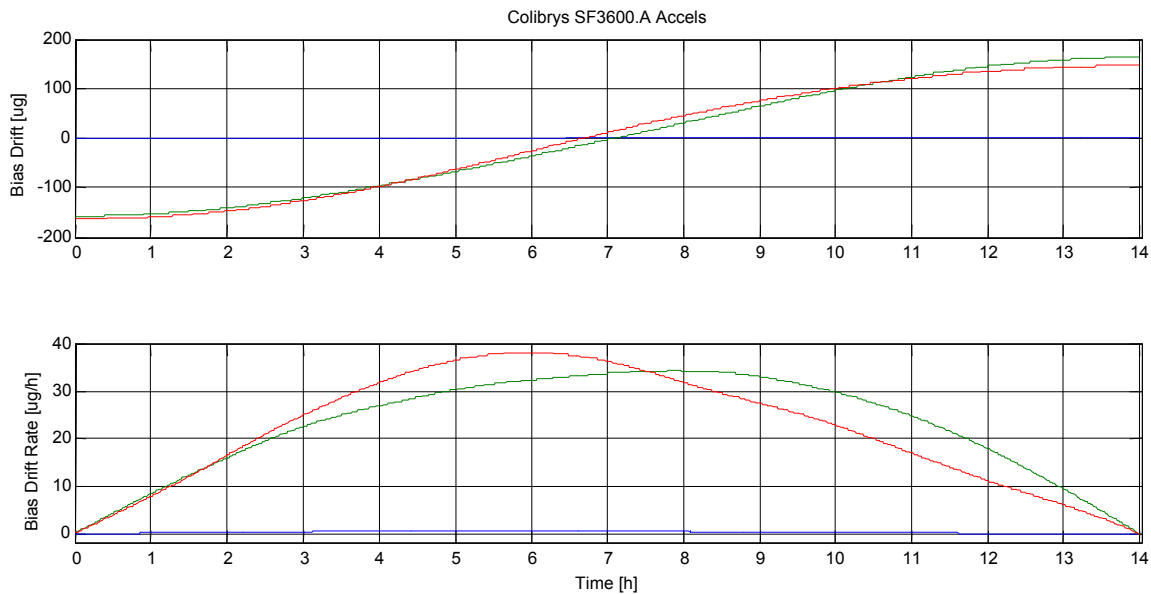


Fig. 6: Long-term Accelerometer Bias Drift Showing a Very Stable Z-Accelerometer

Label Benchmarking: So far, it can be seen that the power supply is a major contributor of the error budget. Figure 5 shows the lab bench testing. The graph in Figure 5 shows that the signal noise is about $16\mu\text{g}/\sqrt{\text{Hz}}$, which equates to $7\mu\text{g}$ at 5 sec filtering time which lead to 500 m spatial resolution (For a 100 m/s moving platform). The power spectral density shows clearly that the noise floor is not completely flat (White) and that a substantial power is contained around 0.45 of the sampling frequency (~ 9 Hz). We are working to resolve this issue at the hardware level to reduce the noise magnitude to less than 1 micro-g. The signal to noise magnitude ratio is 100 dBHz (10^5), though the long-term stability of the Z-Accelerometer over 24 hours of operation seems to be under 1 micro-g per hour, as shown in Figure 6.

CONCLUSION

In this research project a theoretical basis for developing a gravity anomalies measuring device is derived. Light weight system components, device construction and necessary interfacing software are developed and lab tested too. The developed gravimeter (Grav-Map) design uses Commercial off-the-shelf (COTS) nano seismic accelerometer and strap-down GNSS-aided IMU; the former is chosen for its low measurement noise density while the latter is used to analytically stabilize the platform and compensate for its motion errors. The modular COTS design allows for easy upgrade of the

system components to suite the platform and the application. Stochastic modeling of the gravity anomaly is used instead of the deterministic approach of causes and effects [13]. The stochastic modeling simplifies the algorithm as it aims at finding relative changes between points as opposed to their estimated absolute values. This in turn allows for high relative precision, required in many applications. The system can be loaded on-board to map underground resources that have effect on gravity value, for example, groundwater change effect. Gravity measurements are used also to detect the geoid; the theoretical best fit surface of the mean-sea level (MSL) [26]. The extension of the MSL into solid earth is the groundwater table, represents the change in groundwater storage. By correlating the gravity signal with the groundwater table will enable detecting groundwater change. In this paper, we present a prototype precision gravimetry system including GNSS-aided inertial navigation system and a nano accelerometer triad sensor set. Simulation studies is performed and preliminary results of estimating the gravity anomalies found to be within 1 mGal as the long-term stability of the Z-Accelerometer over 24 hours of operation seems to be under 1 micro-g per hour and very stable with stdev 0.016 mgal/sqrt(Hz). It realized stdev of 0.027 and 0.020 mgal/sqrt(Hz) for X and Y directions respectively. Simulation and preliminary bench testing showed the potential of the system design to achieve the target objective. A 1 micro-g gravity disturbance/anomaly

seems to be achievable with this small and light-weight gravimetry system suitable to be boarded on a vehicle or UAS. The signal noise was about $7\mu\text{g}$ at 5 sec filtering (500 m spatial resolution for a 100 m/s moving platform).

As a pilot application, the gravity anomalies measured by the developed Grav-Map device for Alriyadh city in Saudi Arabia were correlated to the underground water depths for the region by El Alfy *et al.* [17] and a correlation of average of 78% is realized. Further system calibration and adjustment using traditional precise gravity measuring instrument will be the next field and lab works. This will be appropriate for each area of application where a reference control points with high accurate gravity measurements are required.

ACKNOWLEDGMENT

This Project was funded by the National Plan for Science, Technology and Innovation (MAARIFAH), King Abdulaziz City for Science and Technology, Kingdom of Saudi Arabia Award Number (SPA 1505).

REFERENCES

1. Creutzfeldt, B., A. Guntner, S. Vorogushyn and B. Merz, 2010. The benefits of gravimeter observations for modelling water storage changes at the field scale, *Journal of Hydrological Earth System Sciences*, 14: 1715-1730.
2. Christie, F.J., 1978. Analysis of gravity data from the Picacho Basin, Pinal County, Arizona, Springfield VA 22161 as PB-290 139.
3. Bruton Alexander, M., 2000. Improving the Accuracy and Resolution of SINS/DGPS Airborne Gravimetry, PhD Dissertation, Geomatics Engineering, University of Calgary, Alberta.
4. Hannah John, 2001. Airborne Gravimetry: A Status Report, Prepared for the Surveyor General Land Information New Zealand.
5. Maurer, D.K., 1985. Gravity survey and depth to bedrock in Carson valley, Nevada-California, USGS Water-Resources Investigations Report 84-4202, OFSS, USGS ox 25425, Lakewood, CO 80225.
6. Watson, K.K., 1987. Gravity drainage analysis for scale heterogeneous porous materials under falling water table conditions, *Water Resources Research Journal*, 23(5) 818-826.
7. Hasan, Shaakeel, Troch, A. Peter, J. Boll and C. Kroner, 2006. Modeling the hydrological effect on local gravity at Moxa, Germany, *Journal of Hydrometeorology*, 7(3): 346-354.
8. Jacob, T., R. Bayer, J. Chery, H. Jourde, N. Moigne, J. Boy, J. Hinderer, B. Luck and P. Brunet, 2008. Absolute gravity monitoring of water storage variation in a karst aquifer on the Larzac plateau (Southern France), *Journal of Hydrology*, 359: 105-117.
9. Pool, D. and M. Anderson, 2008. groundwater storage change and land subsidence in Tucson basin and Avra valley, south-eastern Arizona 1998–2002, USDOI and USGS report 2007-5275.
10. Niu Guo-Yue, 2007. Development of a simple groundwater model for use in climate models and evaluation with Gravity Recovery and Climate Experiment (GRACE) data, *Journal of Geophysical Research*, 112:d7.
11. Seo, K.W., 2006. Terrestrial water mass load changes from Gravity Recovery and Climate Experiment (GRACE), *Water resources research Journal*, 42: 5.
12. Swenson, S., P. Yeh, J. Wahr and J. Famiglietti, 2006. A comparison of terrestrial water storage variations from GRACE with in situ measurements from Illinois, *Geophysical Research Letters*, 33: L16401.
13. Culek, T.E. and D. F. Palmer, 1987. Gravity modeling of the Brimfield township buried valley and associated aquifer, Portage County, Ohio, *Journal of Ground Water*, 25(2): 167-175.
14. Glennie Craig, L., 1999. An Analysis of Airborne Gravity by Strap-down SINS/DGPS, PhD Dissertation, Geomatics Engineering, University of Calgary, Alberta.
15. Pinto, R., J. Kain and A. Mohamed, 2010. Precision Gravimetry Sensing, Enpoint Final Report - NSF Solicitation 09-541: Topic IC3.I.ii NSF Award Number: IIP-0945001.
16. Gehman Carter, 2009. Estimating specific yield and storage change in an unconfined aquifer using temporal gravity surveys, *Water resources research Journal*, 45(0).
17. El-Alfy, M., I. ElSebaie, A. Aguib, A. Mohamed and Q. Tarawneh, 2016. Assessing Groundwater Geospatial Variation Using Microgravity Investigation in the Arid Riyadh Metropolitan Area, Saudi Arabia: a Case Study". *WaterResour Manage DOI 10.1007/s11269-016-1392-9*, 2016.

18. Jekely Christopher, 2000. Inertial Navigation Systems with Geodetic Applications, SLR, ISBN-13: 978-3110159035.
19. Mohamed Ahmed, H., 1999. Optimizing the Estimation Procedure in INS/GPS Integration for Kinematic Applications, PhD Dissertation, Geomatics Engineering, University of Calgary, Alberta.
20. Schwarz, K.P. and M. Wei, 1994. Some Unsolved Problems in Airborne Gravimetry, Proceedings of the International Association of Geodesy Symposium 113, Gravity and Geoid, Springer, Berlin, pp: 131-150.
21. Wei, M. and K.P. Schwarz, 1994. An Error Analysis of Airborne Vector Gravimetry, Proceedings of the International Symposium on Kinematic Systems in Geodesy, Geodynamics and Navigation, Banff, Alberta, pp: 509-520.
22. Grav, D., 2007. Project, Gravity for the Redefinition of the American Vertical Datum, the US NGS NOAA.
23. Hare, J., 2008. The 4D microgravity method for water flood surveillance: Part IV -- modeling and interpretation of early epoch 4D gravity surveys at Prudhoe Bay, Alaska, Journal of Geophysics, 73(6): (WA173).
24. Konikow, L. and E. Kendy, 2005. Groundwater depletion: a global problem, Journal of Hydrogeology, 13: 317-320.
25. Savage Paul, G., 2000. Strap-down Analytics, Strap-down Associate, Inc., Maple Plain, Minnesota.
26. Virtanen, H., M. Nordman, M. Bilker-Koivula, J. Mäkinen and J. Virtanen, 2007. Gravity variation due to hydrology at Metsahovi, Finland, American Geophysical Union, Oct.